

vEEGNet: learning latent representations to reconstruct EEG raw data via variational autoencoders

Alberto Zancanaro¹[0000-0002-5276-7030], Giulia Cisotto^{1,2}[0000-0002-9554-9367],
Italo Zoppis²[0000-0001-7312-7123], and Sara Lucia
Manzoni²[0000-0002-6406-536X]

¹ Department of Information Engineering, University of Padova,
via Gradenigo 6/b, Padova, Italy
`alberto.zancanaro.1@phd.unipd.it`

² Department of Informatics, Systems, and Communication, University of
Milan-Bicocca,
viale Sarca 336, Milan, Italy
`{giulia.cisotto, italo.zoppis, sara.manzoni}@unimb.it`

Abstract. Electroencephalographic (EEG) data are complex multi - dimensional time - series which are very useful in many different applications, i.e., from diagnostics of epilepsy to driving brain-computer interface systems. Their classification is still a challenging task, due to the inherent within- and between-subject variability as well as their low signal-to-noise ratio. On the other hand, the reconstruction of raw EEG data is even more difficult because of the high temporal resolution of these signals. Recent literature has proposed numerous machine and deep learning models that could classify, e.g., different types of movements, with an accuracy in the range 70% to 80% (with 4 classes). On the other hand, a limited number of works targetted the reconstruction problem, with very limited results. In this work, we propose vEEGNet, a DL architecture with two modules, i.e., an unsupervised module based on variational autoencoders to extract a latent representation of the multi-channel EEG data, and a supervised module based on a feed-forward neural network to classify different movements. Furthermore, to build the encoder and the decoder of VAE we exploited the well-known EEGNet network, specifically designed since 2016 to process EEG data. We implemented two slightly different architectures of vEEGNet, thus showing state of the art classification performance, and the ability to reconstruct both low frequency and middle-range components of the raw EEG. Although preliminary, this work is promising as we found out that the low-frequency reconstructed signals are consistent with the so-called motor-related cortical potentials, very specific and well-known motor-related EEG patterns and we could improve over previous literature by reconstructing faster EEG components, too. Further investigations are needed to explore the potentialities of vEEGNet in reconstructing the full EEG data, to generate new samples, and to study the relationship between classification and reconstruction performance.

Keywords: AI · deep learning · variational autoencoder · EEG · machine learning · CNN · latent space · inter-subject variability · time-series · reconstruction · complex systems.

1 Introduction

Classification and reconstruction of raw electroencephalographic data (EEG) are critical tasks that machine learning (ML), and especially deep learning (DL), are asked to solve as this could help in many applications, e.g., from neuroscience to brain-computer interface (BCI), to support the diagnosis of neurological pathologies and the development of new rehabilitation protocols [10,28,36]. Both tasks involve solving a number of challenges, mostly relating to the high temporal resolution of the EEG data, their inherent variability within- and between individuals, as well as their very low signal-to-noise ratio (SNR) [11,9]. The ability of a ML/DL models of extracting the most informative and compact representation of the rich and high-dimensional EEG input dataset, i.e., a latent representation, plays a key role to both obtaining an effective classification and accurately reconstruct the data. Not only these two tasks, but also generation, compression, and denoising might be enabled by such models.

The variational autoencoder (VAE) is a variant of the standard auto-encoder model which consists of an effective encoding-decoding DL architecture that projects data on a *structured* latent space [15]. VAEs have been recently and successfully implemented for a number of unsupervised and semi-supervised learning problems, e.g., including latent feature extraction for further classification [15,13,22,40]. On the other hand, since 2016, convolutional neural networks (CNN) have been successfully exploited for EEG classification in the popular EEGNet architecture [18] and its several later variants. EEGNet is a 2-block architecture that implements both temporal and spatial convolutions and has been consistently shown to outperform earlier ML models for EEG classification [14,39].

Therefore, we directed our efforts in the investigation of the potentialities of the combination of VAE and EEGNet to reach good classification and reconstruction quality, at the same time, for EEG data. In our previous conference paper [41], we proposed *vEEGNet*, an architecture that combined a VAE, i.e., to extract artificial features, with a feed-forward neural network (FFNN), i.e., to classify the data into 4 different motor imagery (MI) classes (the imagination of a right or left hand, the movement of both feet or the tongue, as acquired in the public *dataset 2a* from the BCI competition IV). We showed that *vEEGNet* can classify with accuracy values at the state of the art and, at the same time, can partially reconstruct the input EEG, as limited to its low frequency components. In the present work, we expand our contribution with two different implementations of *vEEGNet*, namely *vEEGNet1* and *vEEGNet2*, showing that *vEEGNet2* has further reconstruction capabilities, i.e., it is able to reconstruct the middle-range components of the raw EEG.

The rest of this paper is organized as follows: Section 2 reports the most relevant related work, Section 3 describes the VAE theory and introduces the general vEEGNet model. Section 4 presents the two different implementations of vEEGNet, the dataset, the classification and reconstruction results with discussion w.r.t. the related state of the art. Finally, section 5 concludes the paper and paves the way toward new promising future directions.

2 State of the art

As EEG is a very noisy data, with a large inherent variability across different subjects and within the same individual, developing a model which is able to reconstruct raw EEG data with very high fidelity is a challenging task, as already shown by literature. For this reason, most related work focused on the classification ability of ML and DL models, but rarely proposed models to specifically reconstructing such type of data. A number of works suggested models and architectures with the primary objective of classifying e.g., movements, emotions, or epileptic seizures, with an inherent, however not deeply exploited, capability of reconstructing EEG. Thus, in this section we summarize the most relevant state of the art with respect to the aim of our work, i.e., both classification and reconstruction of EEG signals during the imagination of movements (MI) [43].

There exist several models to classify EEG of imagined movements. Filter-bank common spatial pattern (FBCSP) [14] is still the most common ML model for classification, especially used in BCI applications. It consists of a 4-step algorithm involving a filter bank with multiple band-pass filters, a spatial filtering via common spatial pattern (CSP), a selection of the most relevant CSP features, and the classification using a standard ML classifier (e.g., support vector machine (SVM)). The well-established literature on this topic reports that this method can achieve up to 80% accuracy in a 4-class MI classification problem [39,33]. Despite its popularity, FBCSP has no reconstruction abilities. Therefore, its main role is barely as baseline comparison with more innovative DL models. Among others, CNN have recently gained a lot of attention as effective architectures for classifying EEG due to their ability to capture both temporal and spatial features. CNN have been particularly used as building blocks for the very successful EEGNet architecture. EEGNet has been presented in 2016 by Lawhern et al. [18] as an architecture to specifically classify raw EEG signals (represented as multi-channel time-series). In its original version, it was made of 2 blocks, each one composed of 2 convolutional layers and a fully-connected layer, and it could barely reach an accuracy of about 70%. However, a number of variants and improvements of EEGNet have been later proposed, further outperforming both the baseline EEGNet as well as FBCSP: among others, Temporary Constrained Sparse Group Lasso enhanced EEGNet (TSGL-EEGNet) [12], Multibranch Shallow CNN (MBSshallow ConvNet) [1], MI-EEGNet [32], Quantized EEGNet (Q-EEGNet) [34], *DynamicNet* [39], and other general-purpose CNN models, namely Channel-wise CNN (CW-CNN) [33], Densely Feature Fusion CNN (DFFN) [20], and the Monolithic Network [29]. They implemented

different pre-processing steps and some of them expanded the baseline EEGNet architecture with stacking multiple EEGNet units (e.g., TSGL-EEGNet and MBSshallow ConvNet), finally reaching accuracy values slightly above 80% in a 4-class MI task.

To further extend the capabilities of DL models to process EEG, some recent architectures based on CNN and autoencoder (AE) were proposed. They were shown to have both classification and basic reconstruction ability. In [23], the authors trained an architecture formed by a CNN that extracted artificial features which were then fed as input to an AE, with the aim of compressing and reconstructing EEG signals corresponding to different emotions (the DEAP [17] and the SEED [42] public datasets were used). After the training, the optimized features were used as input to a FFNN. The latter was used to classify low/high valence levels and low/high arousal levels, separately, in the DEAP dataset, achieving an accuracy of 89.49% for the valence and of 92.86% for the arousal, respectively (w.r.t. a chance level of about 50%). On the other hand, a 3-class classification problem (i.e., to discriminate positive, neutral, or negative emotional conditions) was the task for the FFNN when applied to the SEED dataset, where it achieved an accuracy of 96.77% (w.r.t. a chance level of about 33%). In [31], the authors presented a denoising sparse autoencoder, i.e. an autoencoder that imposes a sparsity condition on the latent space, to learn features from EEG for seizure detection. The learned features were then classified using a linear regression with very satisfactory classification results, i.e., 100% accuracy on the dataset they used [2], both in binary and 3-class classification. Despite the high classification performance and the use of an architecture with the potentiality of reconstructing the input data, the authors did not report any investigation on this aspect. More recently, [4] proposed EEG2VEC, a VAE based architecture that encoded emotions-related EEG data. In this work, for the first time, the latent representation produced by a VAE was used to reconstruct EEG. Interestingly, the authors succeeded in partially reconstructing the low-frequency shape of the signal, but not its entire frequency content, as well. In addition, the amplitude of the reconstructed data was about half that of the input one. Incidentally, we also report that several works have recently used generative adversarial network (GAN) to generate new synthetic EEG samples of MI, i.e., to increase the size of the EEG datasets and, thus, the classification performance of DL-based classifiers [26,25,37]. However, even though interesting and promising, this line of literature mainly addressed the classification problem, providing a substantially different approach from the one that is proposed in this work.

Thus, since our previous work [41], we have directed our attention on the combination of VAE and EEGNet. Specifically, we proposed *vEEGNet*, a VAE-based DL architecture consisting of two learning modules, i.e., an unsupervised representation learning module, and a supervised module, with the aim of both classifying MI EEG data and reconstructing them. The first module was formed by a VAE [15,40,22], while the second by an FFNN. In the VAE, we exploited EEGNet as the glsvae encoder (and, conversely, its mirrored version as the VAE

decoder) to extract a compact and highly informative representation of the EEG (with a latent space of dimension $d = 16$). The latter was later used by the FFNN to classify the EEG into four different classes of movement. At the same time, that representation was used by the decoder to reconstruct the EEG input data. vEEGNet implemented a joint training of the two modules, by minimizing the joint loss function given by the sum of the VAE loss and the classifier loss. Using such architecture, we were able to obtain classification performance at the state of the art and to reconstruct the low-frequency components of the input EEG (in line with [4]).

Therefore, in this work, we decided to extend our previous work by modifying the vEEGNet architecture (i) to create *vEEGNet1*, i.e., very similar to our original vEEGNet but with a larger latent space ($d = 64$), and (ii) to propose *vEEGNet2*, which expands the original vEEGNet’s encoder architecture to make it able to reconstruct not only the low frequency components of the input EEG, but also the higher frequency ones (relevant for the studies on motor control) [30].

3 Methods

3.1 Variational Autoencoder

The VAE is a variant of the standard auto-encoder model which takes advantage of an effective encoding-decoding DL approach to obtain a projection of the data on a *structured* latent space. In fact, VAEs have been recently and successfully implemented for a number of unsupervised and semi-supervised learning problems, e.g., random sampling and interpolation [15,13,22,40].

In mathematical terms, the VAE is trained to learn two different probability distributions: a variational (approximate posterior) distribution $q_\phi(\mathbf{z}|\mathbf{x})$ of latent variables \mathbf{z} , given the observations \mathbf{x} (i.e., at the encoder), as well as a generative model $p_\theta(\mathbf{x}|\mathbf{z})$ (i.e., at the decoder) [6]. This task is accomplished by the aforementioned pair of encoder-decoder networks, parameterized by ϕ and θ , respectively. The VAE training aims to minimizing the VAE loss, \mathcal{L}_{VAE} , w.r.t. the parameters ϕ and θ . \mathcal{L}_{VAE} is usually expressed in term of the Evidence Lower Bound (ELBO) for the (evidence) probability $p(\mathbf{x})$, i.e., $\mathcal{L}(\theta, \phi; \mathbf{x})$: $\mathcal{L}_{VAE} = -\mathcal{L}(\theta, \phi; \mathbf{x})$, provided that

$$\mathcal{L}(\theta, \phi; \mathbf{x}) = \mathbb{E}_{q_\phi(\mathbf{z}|\mathbf{x})} \left(\log \frac{p_\theta(\mathbf{x}, \mathbf{z})}{q_\phi(\mathbf{z}|\mathbf{x})} \right). \quad (1)$$

Thus, for the VAE training, the minimization of \mathcal{L}_{VAE} leads to the maximization of the ELBO for $p(\mathbf{x})$. The gap between $p(\mathbf{x})$ and $\mathcal{L}(\theta, \phi; \mathbf{x})$ can be best expressed by considering the Kullback-Leibler divergence (\mathcal{KL}) between the variational $q_\phi(\mathbf{z}|\mathbf{x})$ and posterior $p_\theta(\mathbf{x}|\mathbf{z})$ distributions, which turns to be

$$\mathcal{KL}[q_\phi(\mathbf{z}|\mathbf{x})||p_\theta(\mathbf{x}|\mathbf{z})] = -\mathcal{L}(\theta, \phi; \mathbf{x}) + p(\mathbf{x}) \quad (2)$$

Since $\mathcal{KL}[q_\phi(\mathbf{z}|\mathbf{x})||p_\theta(\mathbf{x}|\mathbf{z})] \geq 0$, one arrives at the lower bound $\mathcal{L}(\theta, \phi; \mathbf{x}) \leq p(\mathbf{x})$. Similarly, the ELBO can be also formulated as

$$\mathcal{L}(\theta, \phi; \mathbf{x}) = \mathbb{E}_q(p_\theta(\mathbf{x}|\mathbf{z})) - \mathcal{KL}[q_\phi(\mathbf{z}|\mathbf{x})||p(\mathbf{z})] \quad (3)$$

$$= \mathcal{L}_R + \mathcal{L}_{KL} \quad (4)$$

In this way, the first term, $\mathcal{L}_R = \mathbb{E}_q(p_\theta(\mathbf{x}|\mathbf{z}))$, can be interpreted as the likelihood of observing the original data given the input, and thus it provides the reconstruction error. On the other hand, the second term, $\mathcal{L}_{KL} = -\mathcal{KL}[q_\phi(\mathbf{z}|\mathbf{x})||p(\mathbf{z})]$, acts as a regularizer, thus penalizing those *surrogate* distributions ($q_\phi(\mathbf{z}|\mathbf{x})$) too far away from the predefined $p(\mathbf{z})$.

It is worth to note that the VAEs are able to provide output distributions that can be used to generate new samples. In this work, we particularly exploits this opportunity by sampling samples from the latent space and using them to classify the different MI movement classes. However, the investigation of the pure generation of new EEG samples is beyond the scope of this article and it deserves a proper, separate, study.

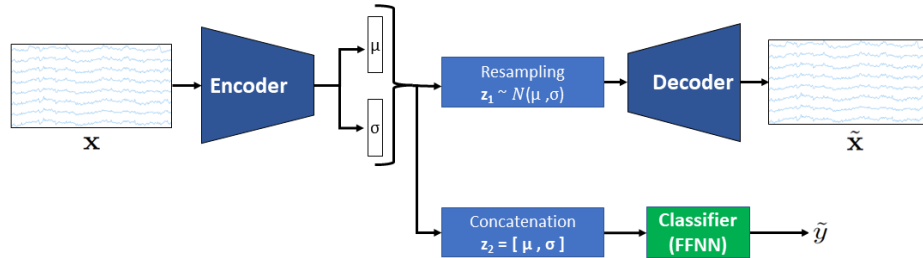


Fig. 1: The general vEEGNet architecture (modified from our previous work [41]).

3.2 vEEGNet general architecture

In this study, we developed a brand-new model which combines the advantages of VAEs [15,22] and the specificity of EEGNet for classify and, at the same time, reconstruct EEG raw data. In our previous works, we have already implemented these architectures for different studies, e.g., a β -VAE for anomaly detection in plants physiology [40], and an efficient version of the well-known EEGNet in [39]. However, here, we combine these two DL models as shown in Fig. 1. Particularly, we implemented EEGNet as one building block of the VAE, i.e., the encoder, and used it to extract a compact representation of the raw EEG data, that can be further projected into a lower dimensional latent space. Then, the VAE decoder consisted of the *mirrored* version of the same EEGNet architecture. To complete the architecture, we added an FFNN which had the aim of classifying

samples extracted from the latent space into one of the classes of interest. Thus, the model consists of two different mechanisms, ruled by an unsupervised and a supervised learning, respectively, as further explained below.

Unsupervised mechanism The unsupervised mechanism exploits the EEGNet architecture to learn both the latent distribution $q_\phi(\mathbf{z}|\mathbf{x})$ as well as the posterior $p_\theta(\mathbf{x}|\mathbf{z})$. For both the prior distribution $p(\mathbf{z})$ and the approximation posterior distribution $q_\phi(\mathbf{z}|\mathbf{x})$, we assumed isotropic Gaussian distribution, i.e.,

$$p(\mathbf{z}) = \mathcal{N}(\mathbf{0}, \mathbf{I}) \quad (5)$$

$$q_\phi(\mathbf{z}|\mathbf{x}) = \mathcal{N}(\mathbf{z}; \mu(\mathbf{x}; \phi), \sigma^2(\mathbf{x}; \phi)\mathbf{I}) \quad (6)$$

where $\mu(\mathbf{x}; \phi)$ and $\sigma(\mathbf{x}; \phi)$ are the functions implemented by the vEEGNet encoder to encode the mean and the (diagonal) covariance matrix of the Gaussian distribution. With these assumptions, $\mathcal{KL}[q_\phi(\mathbf{z}|\mathbf{x})||p(\mathbf{z})]$ (the regularization term defined in Section 3.1) can be directly expressed in the compact analytical form:

$$\mathcal{L}_{KL} = \mathcal{KL}[q_\phi(\mathbf{z}|\mathbf{x})||p(\mathbf{z})] = \frac{1}{2} \sum_{i=1}^d (\sigma_i^2 + \mu_i^2 - 1 - \log(\sigma_i^2)) \quad (7)$$

where μ_i and σ_i^2 are the predicted mean and variance values of the corresponding i -th latent component of \mathbf{z} [15]. The vEEGNet encoder implements a standard EEGNet with its usual blocks, i.e., a temporal convolution, a spatial convolution, and a separable convolution. Lastly, the output is flattened and given to a fully-connected layer. From the vEEGNet encoder’s output (i.e., giving $q_\phi(\mathbf{z}|\mathbf{x})$), we sampled a vector, say \mathbf{z}_1 (using the reparametrization trick $\mathbf{z}_1 = \mu + \sigma \cdot \mathcal{N}(\mathbf{0}, \mathbf{1})$). Then, \mathbf{z}_1 is input to the vEEGNet decoder which had the ultimate goal to reconstruct the original raw EEG signal. The decoder architecture mirrors that of the encoder, i.e., with a sequence of layers made by a separable convolution, a spatial filter, a temporal filter. Transposed convolutions are used instead of normal convolutions, and up-sample layers in place of standard pooling layers. In both the encoder and the decoder, batch normalization and dropout layers were added to increase performance and stability during training. To compute the reconstruction loss during the training, we computed \mathcal{L}_R through the mean square error (MSE).

Supervised mechanism The supervised mechanism is given by the FFNN which aimed at classifying the raw EEG into n different classes, with n the specific number of classes given by the dataset. In vEEGNet, a second vector $\mathbf{z}_2 = [\boldsymbol{\mu}, \boldsymbol{\sigma}^2]$ is obtained by concatenating the output of the encoder, i.e., the parameters vectors $\tilde{\boldsymbol{\mu}} = \mu(\mathbf{x}; \phi)$ and $\tilde{\boldsymbol{\sigma}} = \sigma(\mathbf{x}; \phi)$. This new vector is fed into the classifier to output the predicted class \tilde{y} . For the classifier, we used the negative log-likelihood loss function defined as:

$$\mathcal{L}_{clf} = -\log(\tilde{\mathbf{y}}) \cdot \mathbf{y} \quad (8)$$

where $\log(\tilde{\mathbf{y}})$ are the log probabilities of the possible labels related to input \mathbf{x} , and \mathbf{y} is a one hot encoded vector of the true labels of input \mathbf{x} .

Finally, vEEGNet aimed to minimize the overall loss function \mathcal{L}_{Total} given by the sum of the VAE loss and the classifier loss (\mathcal{L}_{clf}), as follows:

$$\mathcal{L}_{Total} = \mathcal{L}_{VAE} + \mathcal{L}_{clf} = \mathcal{L}_R + \mathcal{L}_{KL} + \mathcal{L}_{clf} \quad (9)$$

4 Results and discussion

4.1 Dataset and vEEGNet implementations

We applied vEEGNet to the public *dataset 2a* of the IV BCI competition [5]. The dataset includes 22-channel EEG recordings from 9 subjects performing imagination of 4 different movements, i.e., the MI of either right or left hand, both feet or tongue. The training set consists of 288 trials (or repetitions) for each subject, while the test set consists of 288 different trials for each subject. The EEG data have been previously filtered with a 0.5 – 100Hz band-pass filter and a notch filter at 50 Hz. We down-sampled the data to 128 Hz, following the same approach of other works [32,18], including our own [39]. Then, for every MI repetition, a 4 s EEG segment was extracted (channel-wise), thus obtaining a 22×512 data matrix.

We implemented vEEGNet in PyTorch ³ and we trained it using RTX 2070, 500 epochs, AdamW optimizer [24], a learning rate of 0.001, and a weight decay of 0.00001. We implemented two slightly, but significantly different, architectures, namely *vEEGNet1* and *vEEGNet2*. They differ in the encoder and the classification network. In vEEGNet1, we simply implemented the original EEGNet [18] as the encoder and its mirrored version as the decoder with a latent space of dimension $d = 64$. The full architecture is shown in detail in Fig. 2. Moreover, the classifier consists of an input layer with 128 neurons, followed by one hidden layer with 64 neurons, and an ELU activation function. The output layer has 4 neurons to classify the 4 different MI tasks and implements a log-softmax activation function. On the other hand, in vEEGNet2, we further expanded the encoder and implemented it as 3 parallel EEGNet networks (i.e., 3 sub-encoders), as inspired by the work of [1]. The decoder remained unchanged. Interestingly, the 3 sub-encoders differed from each other by the length of the kernels in the first layer, i.e., the layer responsible for time convolutions. In fact, using temporal kernels with different lengths makes it possible to specialize each sub-encoder in learning features with different frequency contents (i.e., different frequency bands). Therefore, we selected the values of 64, 16 and 4, respectively, for the kernel lengths of the 3 sub-encoders. Finally, the vEEGNet2 classifier consists of an input layer with 128 neurons, followed by an output layer with 4 neurons (with the log-softmax activation function kept to obtain the classification and no hidden layers). To note, we trained vEEGNet2 using the min-max

³ The code is available on GitHub: https://github.com/jesus-333/Variational-Autoencoder-for-EEG-analysis/tree/code_ICT4AWE_2023

normalized EEG data, i.e., with values in the range $[-1, 1]$, as we observed an improvement of its reconstruction ability.

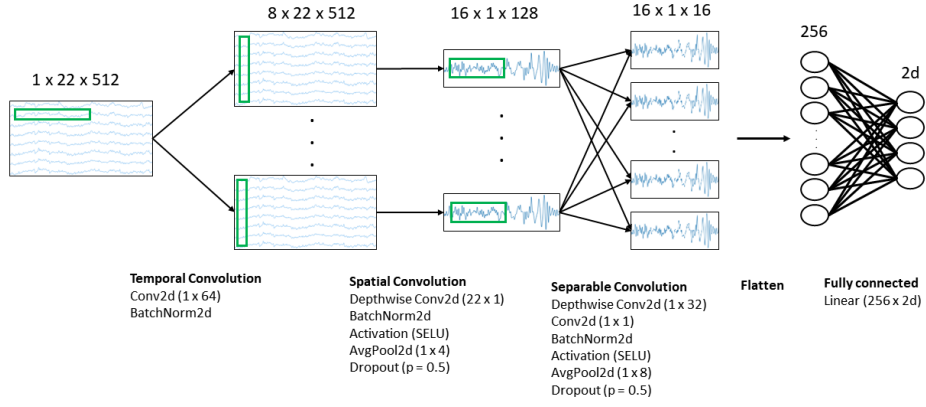
The total number of trainable parameters for vEEGNet1 is 61476, with 52960 of them for the implementation of the unsupervised mechanism and the remaining 8516 for the supervised one. On the other hand, the total number of trainable parameters for vEEGNet2 is 121853, with 516 parameters belonging to the architecture part that implements the classifier. Note that the decreased number of parameters for vEEGNet2 classifier is due to the absence of any hidden layer in the classifier. To note, for both implementations, from our previous empirical evaluations [41], we chose $d = 64$ as the hidden space dimension for the latent space extracted by the encoder. In line with a common empirical approach, and with previous works, including ours [38,41], we considered the first $d/2$ neurons as the vector of the means ($\boldsymbol{\mu}$), and the remaining $d/2$ neurons as the vector of the variances ($\boldsymbol{\sigma}^2$).

4.2 vEEGNet performance

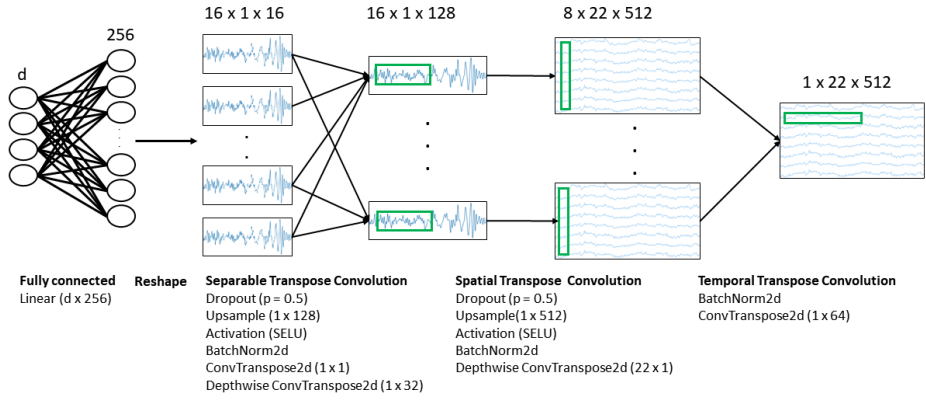
Both vEEGNet1 and vEEGNet2 were evaluated for their classification and reconstruction abilities on the *dataset 2a*. Particularly, vEEGNet1 was able to classify the 4 different imagined movements with a performance in line with the most recent state of the art. Table 1 reports the classification accuracy and the Cohen’s κ score obtained by vEEGNet1 for every subject. The performance of other relevant and recent DL models are reported as a comparison, including the authors’ previous EEGNet implementation through *DynamicNet* (a tool to facilitate the implementation of neural networks [39]). Only models classifying all 4 types of movements were included in this comparison (i.e., with a chance level of 0.25). From these results, it is possible to notice how the inter-subject inherent variability influenced the classification of the different models.

As from the classification results reported in Table 1, we observed that those models which combine multiple EEGNet *units* (e.g., TSGL-EEGNet, MBShallow ConvNet) can reach higher performance (up to 80%, with improvements of 2-8% w.r.t. to the other models), we implemented vEEGNet2. Unfortunately, vEEGNet2 did not improve the classification performance as expected, e.g., barely reaching a maximum accuracy value for 64.58 for subject 1.

Nevertheless, as the reconstruction task as regards, both vEEGNet1 and vEEGNet2 showed their own potentialities and specificity. Fig. 3 reports an example of EEG signal (channel C3, right-hand MI) as reconstructed by vEEGNet1 (Fig. 3(a)) and vEEGNet2 (Fig. 3(b)), respectively. In fact, from the reconstruction obtained by vEEGNet1, we recognize the so-called motor related cortical potential (MRCP), a specific and well-known EEG component that typically appears when a movement is executed or imagined. MRCPs are low-frequency components (in the range of 0.5-4 Hz) that are characterized by a sequence of a positive peak occurring right after the beginning of the movement, a negative peak (within 1 s), and finally a rebound to positive values. The MRCP tends to expire (i.e., return to baseline values) within approximately 2 s after the beginning of the movement. Therefore, in Fig. 3 (a), we could observe a pattern



(a) Encoder.



(b) Decoder

Fig. 2: The vEEGNet1 architecture, with all implementation details (i.e., parameters and activation functions).

Table 1: Comparison of vEEGNet1 with other DL models in terms of classification accuracy ([%]) and kappa score (when available, its value is within brackets) in a 4-class MI task. The first five columns refer to EEGNet-based models, while the last three columns refer to general-purpose CNN models. AVG stands for average, STD for standard deviation. The table was slightly modified from our original conference paper [41].

	vEEGNet1 (d = 64)	EEGNet	TSGL- EEGNet	MI-EEGNet	MBSHallow ConvNet	CW-CNN	DFFN	Monolithic Network
1	70.83	81.88	85.41 (0.81)	83.68 (0.78)	82.58 (0.77)	86.11 (0.82)	83.2	83.13 (0.67)
2	57.64	60.97	70.67 (0.61)	49.65 (0.33)	70.01 (0.6)	60.76 (0.48)	65.69	65.45 (0.35)
3	85.76	88.54	95.24 (0.94)	89.24 (0.86)	93.79 (0.92)	86.81 (0.82)	90.29	80.29 (0.65)
4	61.46	70.63	80.26 (0.74)	68.06 (0.57)	82.6 (0.77)	67.36 (0.57)	69.42	81.6 (0.62)
5	60.42	68.45	70.29 (0.6)	64.93 (0.53)	77.81 (0.7)	62.5 (0.5)	61.65	76.7 (0.58)
6	62.85	61.46	68.37 (0.58)	56.25 (0.42)	64.79 (0.53)	45.14 (0.27)	60.74	71.12 (0.45)
7	71.88	82.08	90.97 (0.88)	94.1 (0.92)	88.02 (0.84)	90.63 (0.88)	85.18	84 (0.69)
8	77.43	82.15	86.35 (0.82)	82.64 (0.77)	86.91 (0.83)	81.25 (0.75)	84.21	82.66 (0.7)
9	65.28	66.25	83.64 (0.79)	82.99 (0.77)	83.38 (0.78)	77.08 (0.69)	85.48	80.74 (0.64)
AVG	68.17	73.60	81.34 (0.75)	74.61 (0.66)	81.15 (0.75)	73.07 (0.64)	76.44	78.1 (0.59)
STD	9.14	10.20	9.61 (0.13)	15.44 (0.21)	9.03 (0.12)	15.11 (0.2)	11.65	6.27 (0.12)

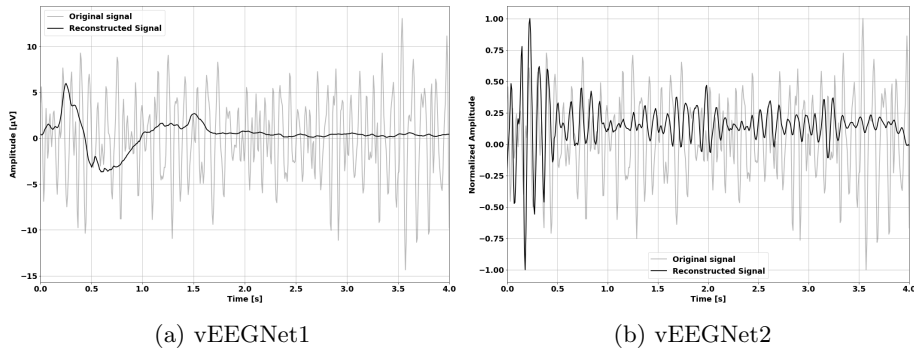


Fig. 3: An example of an EEG signal (channel C3, right-hand MI) as reconstructed by (a) vEEGNet1 and (b) vEEGNet2.

that is very consistent with the one expected by the literature [27,21,8]. On the other hand, vEEGNet2 showed the ability to reconstruct middle-range frequency components (approximately in the range 5-20 Hz). Both frequency bands, i.e., the low and the middle range, have a critical importance in neuroscience studies related to movement [8] and, as such, both vEEGNet1 and vEEGNet2 have their own potentialities to be useful in this context. Fig. 4 shows four different reconstructed EEG channels, namely C3, C4, Cz, and the average of FC3 and FC4, selected based on their relevance to the MI tasks. In line with well-known literature [19], the most relevant electrodes where to retrieve information related to the hand movement (i.e., target sensors) are C3 and C4, for the movements of the right and the left hand, respectively, Cz for the feet, and sensors F3 and F4 for the tongue. Since, F3 and F4 were not available in this dataset, then we considered the nearest available sensors which were FC3 and FC4 (based on the International 10-20 System for EEG electrode placement). As expected from the literature [35], all reconstructed signals from the target sensors displayed the MRCP and are suitable for a further neurophysiological investigation. However, it is possible to note that both architectures are not fully able to reconstruct the entire 4s EEG segments. Specifically, they can follow the raw data behaviour with high-fidelity in the initial part (actually, very critical to study movement initiation [7,16]), but then the reconstructed signals vanish. Also, the output from vEEGNet2 has been magnified to the range of $[-1, 1]$ to have a scale that is comparable with the raw data (i.e., scaled in the same range as explained above). These issues represent limitations of our architectures that deserve further investigations. However, other works have recently showed similar problems in reconstructing EEG signals. As an example, in [4], the authors used an EEGNet-based VAE to encode and then reconstruct the EEG data related to emotions. They succeeded in reconstructing only a low-frequency signal. In addition, the amplitude of the reconstructed signal was about half that of the original one. [3] used a VAE to generate steady-state visual evoked potentials (SSVEP)-related EEG data at 3 different frequencies, i.e., 10 Hz, 12 Hz, and 15 Hz. The reconstructed signals resembled the original ones but their amplitude was much smaller.

To further evaluate the reconstruction capability of both vEEGNet1 and vEEGNet2, we also report the average reconstruction error for the two different implementations. Tab. 2 and Tab. 3 show the average (across segments) of the MSE computed between every raw 4s EEG segment and its reconstructed version, subject-wise. The values are independently reported for the training and the test set, respectively. As expected, it can be observed (e.g., Tab. 2) the high variability of the reconstruction quality for different subjects (with MSE values ranging between 17.23 and 84.19 in the training set and from 21.71 to 84.72 in the test set). Also, we can further notice that some subjects have a higher degree of inherent intra-subject variability, with large standard deviations compared to the average (e.g., subjects 2 in the test set). This might have increased the difficulty in reconstructing high-quality EEG signals. Incidentally, we might speculate that in cases such that of subject 2, i.e., when there is a huge difference

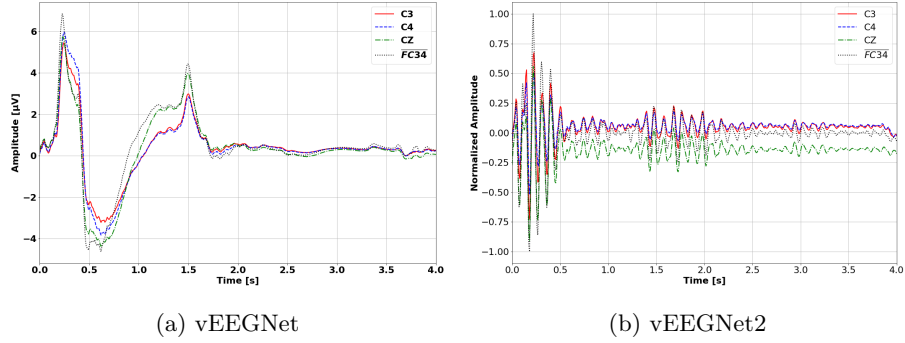


Fig. 4: An example of 4 different EEG signals from 4 target sensors (namely, C3, C4, Cz, and the average between FC3 and FC4) as reconstructed by (a) vEEGNet and (b) vEEGNet2. Panel (a) has been reported from our previous conference paper [41] to show the difference with the results from vEEGNet2.

Table 2: Reconstruction error for vEEGNet1

Subject	Train set		Test set	
	AVG	STD	AVG	STD
1	27.82	5.79	28.22	5.75
2	29.30	6.20	66.13	54.88
3	50.16	15.37	47.55	13.70
4	24.63	4.62	26.31	6.01
5	17.23	3.26	21.71	4.10
6	48.46	13.12	44.04	13.07
7	22.33	4.68	27.71	5.95
8	80.76	22.17	70.49	15.32
9	84.19	23.64	84.72	27.86
AVG	42.76		46.32	
STD	10.98		16.29	

between the test and training set results, overfitting might have been occurred. Alternatively, the high standard deviation might equally be due to the presence of anomalies (due to the recording setup as well as the physiological condition of the subject) that greatly increase the variability of the EEG data and, consequently, make it more difficult to accurately reconstruct the signals. Despite the different ranges for the average MSE values (due to the normalization operated in vEEGNet2), we can see from Tab. 3 that the results obtained from vEEGNet2 are far more robust. The EEG of all subjects can be reconstructed with an average MSE which is about 0.11 with a small standard deviation (about one order of magnitude smaller than the corresponding average value). Moreover, the performance in the test set are rather comparable with the training set, with no cases of significant drop of the reconstruction quality.

Table 3: Reconstruction error for vEEGNet2

Subject	Train set		Test set	
	AVG	STD	AVG	STD
1	0.112	0.013	0.115	0.012
2	0.111	0.015	0.118	0.015
3	0.113	0.015	0.117	0.015
4	0.111	0.013	0.111	0.013
5	0.097	0.016	0.097	0.015
6	0.112	0.012	0.112	0.013
7	0.108	0.012	0.107	0.013
8	0.117	0.013	0.115	0.012
9	0.118	0.014	0.122	0.013
AVG	0.111		0.113	
STD	0.006		0.007	

5 Conclusions

In this work, we tackled the challenging task of developing a DL model which is both able to classify different types of EEG data, e.g., different types of imagined movements (MI), and to reconstruct the raw EEG signals with high fidelity. Providing a solution to these challenges would have such a great impact in many different applications, e.g., from denoising to data generation in neuroscience and BCI.

After reviewing the related work, we directed our efforts on developing an architecture which combines the reconstructing and generative potentialities of the VAE models with the well-known CNN-based EEGNet model, which has been specifically created to process EEG data, namely vEEGNet, which have preliminarily been proposed in our previous conference paper.

In this work, we presented two different implementations of vEEGNet, namely vEEGNet1 and vEEGNet2, and we applied them to a well-known public 22-channel EEG dataset, i.e., the *dataset 2a* from the IV BCI competition, to both classify 4 different types of imagined movements and reconstruct them. We showed that vEEGNet1 is able to reach state of the art accuracy values in the classification task (around 70% w.r.t. a chance level of 25%) and to reconstruct a low-frequency component from the input data. Interestingly, we have recognized such a component as the well-known physiological phenomenon called MRCP. To improve the reconstruction performance and inspired by recent literature, we further expanded vEEGNet into vEEGNet2, which implemented 3 parallel EEGNet networks to form its encoder. Thus, with this design choice, we were able to capture faster EEG components and reconstruct them. With vEEGNet2, we were able to significantly overcome the limitations of other previous works [4,41] which proposed DL architectures that could reconstruct low-frequency components, only.

Overall, vEEGNet in its two implementations achieved good classification results and promising reconstruction performance, improving the state of the art. However, this contribution is still preliminary and, as such, a number of limitations and open challenges are also discussed, and will need further investigations. Among others, from this work we found out that achieving a good classification accuracy does not necessarily means to have a good quality reconstruction, i.e., as observed from the classification results of vEEGNet2. However, this is in line with other works, e.g., the EEG2VEC [4] showed a very good classification performance, at the expenses of a rather limited quality in the reconstruction. Furthermore, future investigations might be also directed to explore the potentialities of vEEGNet (and its different implementations) as generative model for EEG in order to cope with the common lack of large EEG datasets thus helping DL models to improve their performance and better generalize over different EEG datasets.

Acknowledgements

This work was partially supported by the MUR under the grant “Dipartimenti di Eccellenza 2023-2027” of the Department of Informatics, Systems and Communication of the University of Milano-Bicocca, Italy.

AZ is also supported by PON 2014-2020 action IV.4 funded by the Italian Ministry of University and Research at the University of Padova (Padova, Italy).

GC is also supported by PON Initiative 2014-2020 action IV.6 funded by the Italian Ministry of University and Research at the University of Milan-Bicocca (Milan, Italy).

References

1. Altuwajjri, G.A., Muhammad, G.: A multibranch of convolutional neural network models for electroencephalogram-based motor imagery classification. *Biosen-*

- sors **12**(1) (2022). <https://doi.org/10.3390/bios12010022>, <https://www.mdpi.com/2079-6374/12/1/22>
2. Andrzejak, R., Lehnertz, K., Mormann, F., Rieke, C., David, P., Elger, C.: Indications of nonlinear deterministic and finite-dimensional structures in time series of brain electrical activity: Dependence on recording region and brain state. *Physical review. E, Statistical, nonlinear, and soft matter physics* **64**, 061907 (01 2002). <https://doi.org/10.1103/PhysRevE.64.061907>
 3. Aznan, N., Atapour Abarghouei, A., Bonner, S., Connolly, J., Al Moubayed, N., Breckon, T.: Simulating brain signals: Creating synthetic eeg data via neural-based generative models for improved ssvep classification. pp. 1–8 (07 2019). <https://doi.org/10.1109/IJCNN.2019.8852227>
 4. Bethge, D., Hallgarten, P., Grosse-Puppenthal, T., Kari, M., Chuang, L.L., Özdenizci, O., Schmidt, A.: Eeg2vec: Learning affective eeg representations via variational autoencoders. In: 2022 IEEE International Conference on Systems, Man, and Cybernetics (SMC). pp. 3150–3157 (2022). <https://doi.org/10.1109/SMC53654.2022.9945517>
 5. Blankertz, B., Dornhege, G., Krauledat, M., Müller, K.R., Curio, G.: The non-invasive Berlin Brain-Computer Interface: Fast acquisition of effective performance in untrained subjects. *NeuroImage* **37**, 539–50 (09 2007). <https://doi.org/10.1016/j.neuroimage.2007.01.051>
 6. Blei, D.M., Kucukelbir, A., McAuliffe, J.D.: Variational inference: A review for statisticians. *Journal of the American statistical Association* **112**(518), 859–877 (2017)
 7. Bodda, S., Diwakar, S.: Exploring eeg spectral and temporal dynamics underlying a hand grasp movement. *Plos one* **17**(6), e0270366 (2022)
 8. Bressan, G., Cisotto, G., Müller-Putz, G.R., Wriessnegger, S.C.: Deep learning-based classification of fine hand movements from low frequency eeg. *Future Internet* **13**(5), 103 (2021)
 9. Cisotto, G., Capuzzo, M., Guglielmi, A.V., Zanella, A.: Feature selection for gesture recognition in internet-of-things for healthcare. In: ICC 2020-2020 IEEE International Conference on Communications (ICC). pp. 1–6. IEEE (2020)
 10. Cisotto, G., Capuzzo, M., Guglielmi, A.V., Zanella, A.: Feature stability and setup minimization for EEG-EMG-enabled monitoring systems. *EURASIP Journal on Advances in Signal Processing* **2022**(1), 103 (2022)
 11. Cisotto, G., Pupolin, S., Silvoni, S., Cavinato, M., Agostini, M., Piccione, F.: Brain-computer interface in chronic stroke: An application of sensorimotor closed-loop and contingent force feedback. In: 2013 IEEE International Conference on Communications (ICC). pp. 4379–4383. IEEE (2013)
 12. Deng, X., Zhang, B., Yu, N., Liu, K., Sun, K.: Advanced TSGL-EEGNet for motor imagery EEG-based Brain-Computer Interfaces. *IEEE Access* **9**, 25118–25130 (2021). <https://doi.org/10.1109/ACCESS.2021.3056088>
 13. Hinton, G.E., Salakhutdinov, R.R.: Reducing the dimensionality of data with neural networks. *science* **313**(5786), 504–507 (2006)
 14. Kai Keng Ang, Zheng Yang Chin, Haihong Zhang, Cuntai Guan: Filter bank common spatial pattern (FBCSP) in Brain-Computer Interface. In: 2008 IEEE Int. Joint Conf. on Neural Networks (IEEE World Congress on Computational Intelligence) (2008)
 15. Kingma, D.P., Welling, M.: Auto-encoding variational bayes. arXiv preprint arXiv:1312.6114 (2013)

16. Kobler, R.J., Kolesnichenko, E., Sburlea, A.I., Müller-Putz, G.R.: Distinct cortical networks for hand movement initiation and directional processing: an eeg study. *NeuroImage* **220**, 117076 (2020)
17. Koelstra, S., Muhl, C., Soleymani, M., Lee, J.S., Yazdani, A., Ebrahimi, T., Pun, T., Nijholt, A., Patras, I.: Deap: A database for emotion analysis ;using physiological signals. *IEEE Transactions on Affective Computing* **3**(1), 18–31 (2012). <https://doi.org/10.1109/T-AFFC.2011.15>
18. Lawhern, V., Solon, A., Waytowich, N., Gordon, S., Hung, C., Lance, B.: EEGNet: A compact convolutional network for EEG-based Brain-Computer Interfaces. *Journal of Neural Engineering* **15** (11 2016). <https://doi.org/10.1088/1741-2552/15/11/11P01>
19. Lazurenko, D., Kirov, V., Aslanyan, E., Shepelev, I., Bakhtin, O., Minyaeva, N.: Electrographic properties of movement-related potentials. *Neuroscience and Behavioral Physiology* **48**(9), 1078–1087 (2018)
20. Li, D., Wang, J., Xu, J., Fang, X.: Densely feature fusion based on convolutional neural networks for motor imagery EEG classification. *IEEE Access* **7**, 132720–132730 (2019). <https://doi.org/10.1109/ACCESS.2019.2941867>
21. Li, H., Huang, G., Lin, Q., et al.: Combining movement-related cortical potentials and event-related desynchronization to study movement preparation and execution. *Frontiers in neurology* **9**, 822 (2018)
22. Li, Y., Pan, Q., Wang, S., Peng, H., Yang, T., Cambria, E.: Disentangled variational auto-encoder for semi-supervised learning. *Information Sciences* **482**, 73–85 (2019)
23. Liu, J., Wu, G., Luo, Y., Qiu, S., Yang, S., Li, W., Bi, Y.: Eeg-based emotion classification using a deep neural network and sparse autoencoder. *Frontiers in Systems Neuroscience* **14** (2020). <https://doi.org/10.3389/fnsys.2020.00043>, <https://www.frontiersin.org/articles/10.3389/fnsys.2020.00043>
24. Loshchilov, I., Hutter, F.: Decoupled weight decay regularization. In: *International Conference on Learning Representations* (2019), <https://openreview.net/forum?id=Bkg6RiCqY7>
25. Luo, T.j., Fan, Y., Chen, L., Guo, G., Zhou, C.: Eeg signal reconstruction using a generative adversarial network with wasserstein distance and temporal-spatial-frequency loss. *Frontiers in Neuroinformatics* **14** (2020). <https://doi.org/10.3389/fninf.2020.00015>, <https://www.frontiersin.org/articles/10.3389/fninf.2020.00015>
26. Luo, Y., Lu, B.L.: Eeg data augmentation for emotion recognition using a conditional wasserstein gan. In: *2018 40th Annual International Conference of the IEEE Engineering in Medicine and Biology Society (EMBC)*. pp. 2535–2538 (2018). <https://doi.org/10.1109/EMBC.2018.8512865>
27. Magnuson, J.R., McNeil, C.J.: Low-frequency neural activity at rest is correlated with the movement-related cortical potentials elicited during both real and imagined movements. *Neuroscience Letters* **742**, 135530 (2021). <https://doi.org/https://doi.org/10.1016/j.neulet.2020.135530>, <https://www.sciencedirect.com/science/article/pii/S0304394020308004>
28. Martiradonna, S., Cisotto, G., Boggia, G., Piro, G., Vangelista, L., Tomasin, S.: Cascaded wlan-fwa networking and computing architecture for pervasive in-home healthcare. *IEEE Wireless Communications* **28**(3), 92–99 (2021)
29. Olivas, B.E., Chacon, M.: Classification of multiple motor imagery using deep convolutional neural networks and spatial filters. *Applied Soft Computing* **75** (11 2018). <https://doi.org/10.1016/j.asoc.2018.11.031>
30. Pfurtscheller, G., Brunner, C., Schlögl, A., Da Silva, F.L.: Mu rhythm (de) synchronization and EEG single-trial classification of different motor imagery tasks. *NeuroImage* **31**(1), 153–159 (2006)

31. Qiu, Y., Zhou, W., Yu, N., Du, P.: Denoising sparse autoencoder-based ictal eeg classification. *IEEE Transactions on Neural Systems and Rehabilitation Engineering* **26**(9), 1717–1726 (2018). <https://doi.org/10.1109/TNSRE.2018.2864306>
32. Riyad, M., Khalil, M., Adib, A.: MI-EEGNET: A novel convolutional neural network for motor imagery classification. *Journal of Neuroscience Methods* **353**, 109037 (2021). <https://doi.org/https://doi.org/10.1016/j.jneumeth.2020.109037>, <https://www.sciencedirect.com/science/article/pii/S016502702030460X>
33. Sakhavi, S., Guan, C., Yan, S.: Learning temporal information for brain-computer interface using convolutional neural networks. *IEEE Transactions on Neural Networks and Learning Systems* **29**(11), 5619–5629 (2018)
34. Schneider, T., Wang, X., Hersche, M., Cavigelli, L., Benini, L.: Q-EEGNet: An energy-efficient 8-bit quantized parallel EEGNet implementation for edge motor-imagery brain-machine interfaces. In: 2020 IEEE International Conference on Smart Computing (SMARTCOMP). pp. 284–289. IEEE (2020)
35. Seeland, A., Manca, L., Kirchner, F., Kirchner, E.A.: Spatio-temporal comparison between erd/ers and mrpc-based movement prediction. In: Proceedings of the International Conference on Bio-inspired Systems and Signal Processing - Volume 1: BIOSIGNALS, (BIOSTEC 2015). pp. 219–226. INSTICC, SciTePress (2015). <https://doi.org/10.5220/0005214002190226>
36. Silvoni, S., Cavinato, M., Volpato, C., Cisotto, G., Genna, C., Agostini, M., Turolla, A., Ramos-Murguialday, A., Piccione, F.: Kinematic and neurophysiological consequences of an assisted-force-feedback brain-machine interface training: a case study. *Frontiers in neurology* **4**, 173 (2013)
37. Tian, C., Ma, Y., Cammon, J., Fang, F., Zhang, Y., Meng, M.: Dual-encoder vae-gan with spatiotemporal features for emotional eeg data augmentation. *IEEE Transactions on Neural Systems and Rehabilitation Engineering* **31**, 2018–2027 (2023). <https://doi.org/10.1109/TNSRE.2023.3266810>
38. Wang, J., Wei, M., Zhang, L., Huang, G., Liang, Z., Li, L., Zhang, Z.: An autoencoder-based approach to predict subjective pain perception from high-density evoked eeg potentials. In: 2020 42nd Annual International Conference of the IEEE Engineering in Medicine and Biology Society (EMBC). pp. 1507–1511 (2020). <https://doi.org/10.1109/EMBC44109.2020.9176644>
39. Zancanaro, A., Cisotto, G., Paulo, J.R., Pires, G., Nunes, U.J.: CNN-based approaches for cross-subject classification in motor imagery: From the state-of-the-art to DynamicNet. In: 2021 IEEE Conference on Computational Intelligence in Bioinformatics and Computational Biology (CIBCB). pp. 1–7 (2021). <https://doi.org/10.1109/CIBCB49929.2021.9562821>
40. Zancanaro, A., Cisotto, G., Tegegn, D.D., Manzoni, S.L., Reguzzoni, I., Lotti, E., Zoppis, I.: Variational autoencoder for early stress detection in smart agriculture: A pilot study. In: 2022 IEEE Workshop on Metrology for Agriculture and Forestry (MetroAgriFor). pp. 126–130. IEEE (2022)
41. Zancanaro, A., Zoppis, I., Manzoni, S., Cisotto, G.: veegnet: A new deep learning model to classify and generate eeg. In: Proceedings of the 9th International Conference on Information and Communication Technologies for Ageing Well and e-Health - Volume 1: ICT4AWE,. pp. 245–252. INSTICC, SciTePress (2023). <https://doi.org/10.5220/0011990800003476>
42. Zheng, W.L., Lu, B.L.: Investigating critical frequency bands and channels for eeg-based emotion recognition with deep neural networks. *IEEE Transactions on Autonomous Mental Development* **7**(3), 162–175 (2015). <https://doi.org/10.1109/TAMD.2015.2431497>

43. Zoppis, I., Zanga, A., Manzoni, S., Cisotto, G., Morreale, A., Stella, F., Mauri, G.: An attention-based architecture for eeg classification. In: BIOSIGNALS. pp. 214–219 (2020)